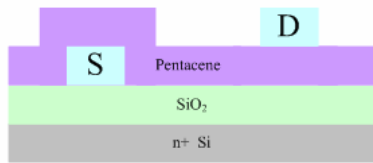


(a)

**TBC bot-source**



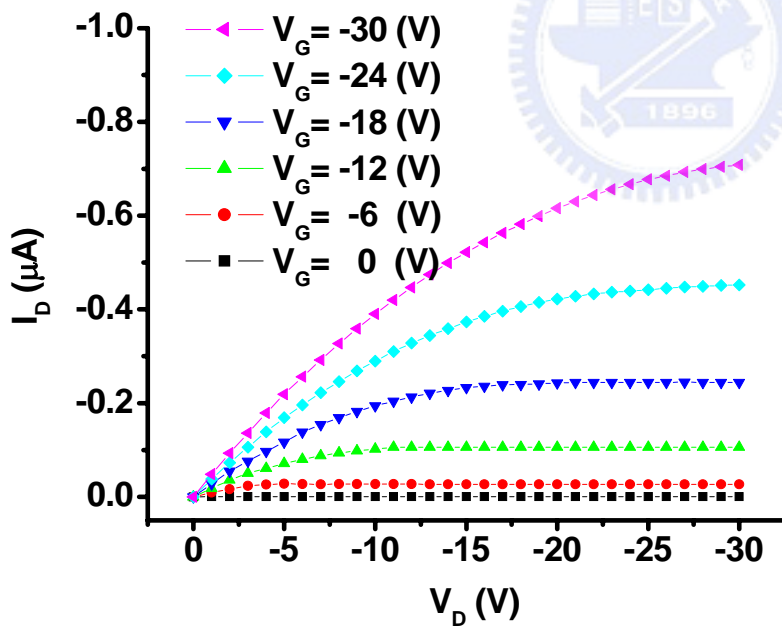
(b)

**TBC top-source**



**Fig. 3.8** Different bias in TBC structures (a) TBC bot-source and (b) TBC top-source

(a)



(b)

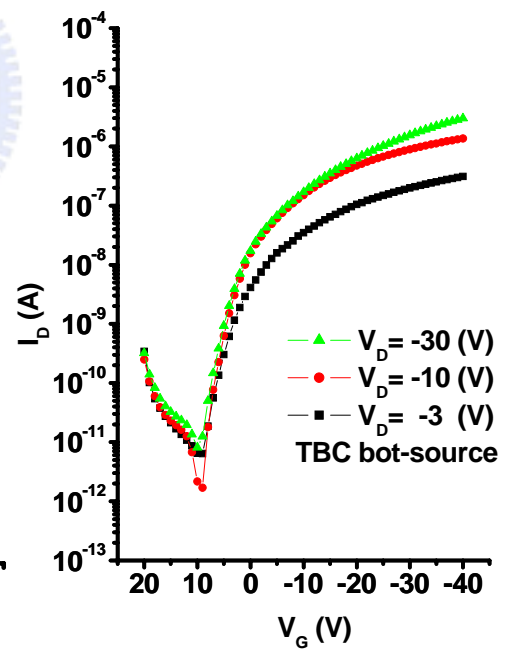


**Fig. 3.9** (a) Output characteristics and (b) transfer characteristics of TBC bottom-source

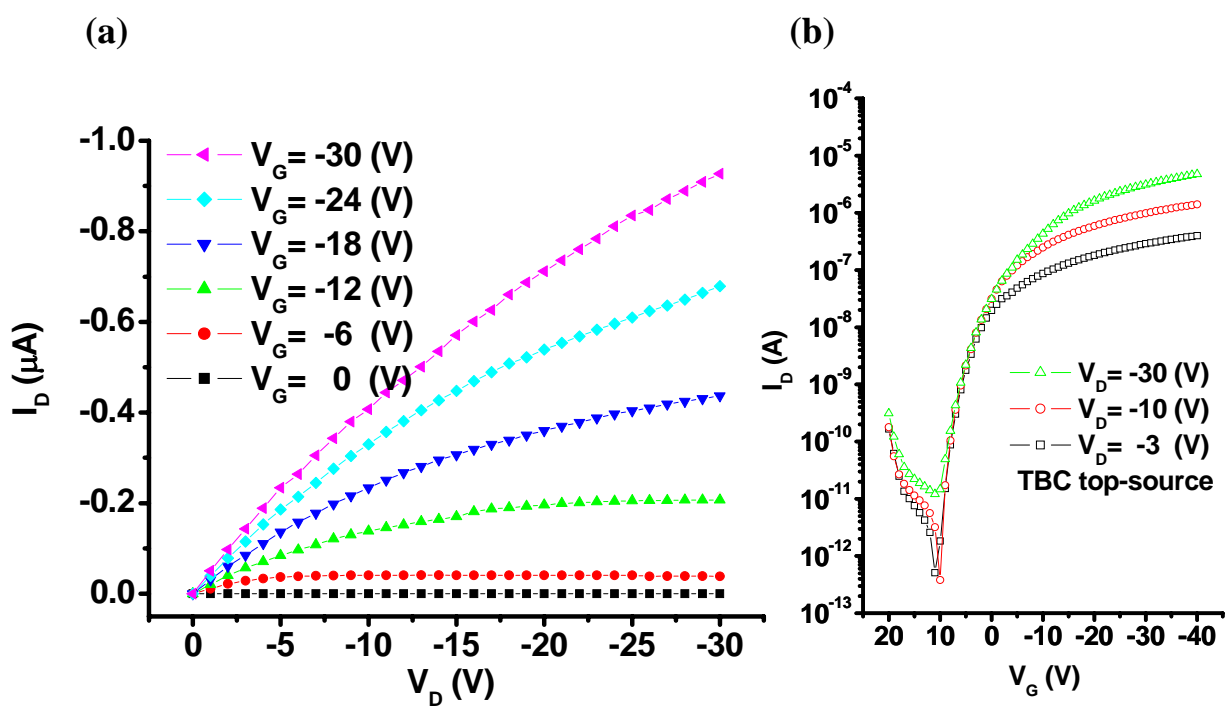


Fig 3.10 (a)Output characteristics and (b) transfer characteristics of TBC top-source

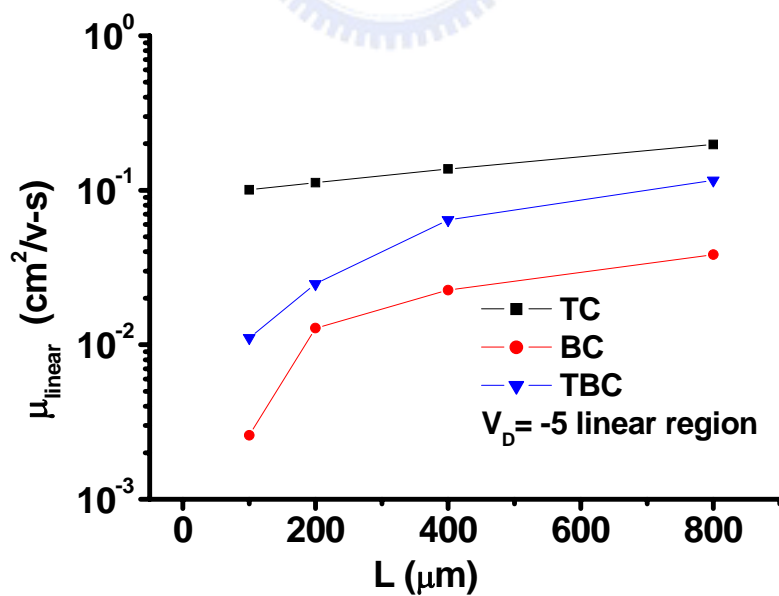
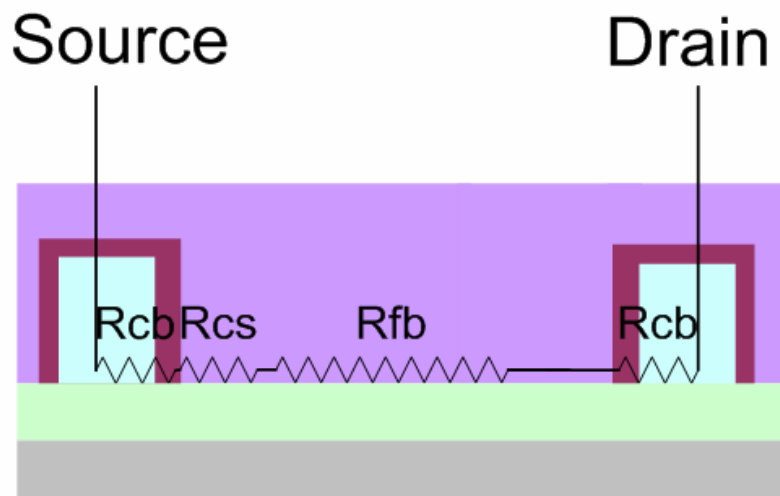
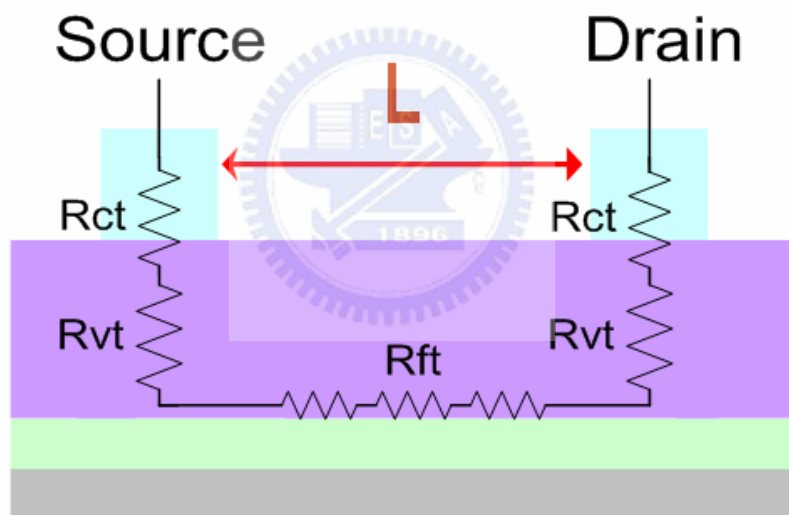


Fig 3.11 Mobility lowering in TC, BC, TBC OTFTs

(a)



(b)



**Fig. 3.12**  $R_{on}$  Modeling in (a) BC OTFTs and (b) TC OTFTs

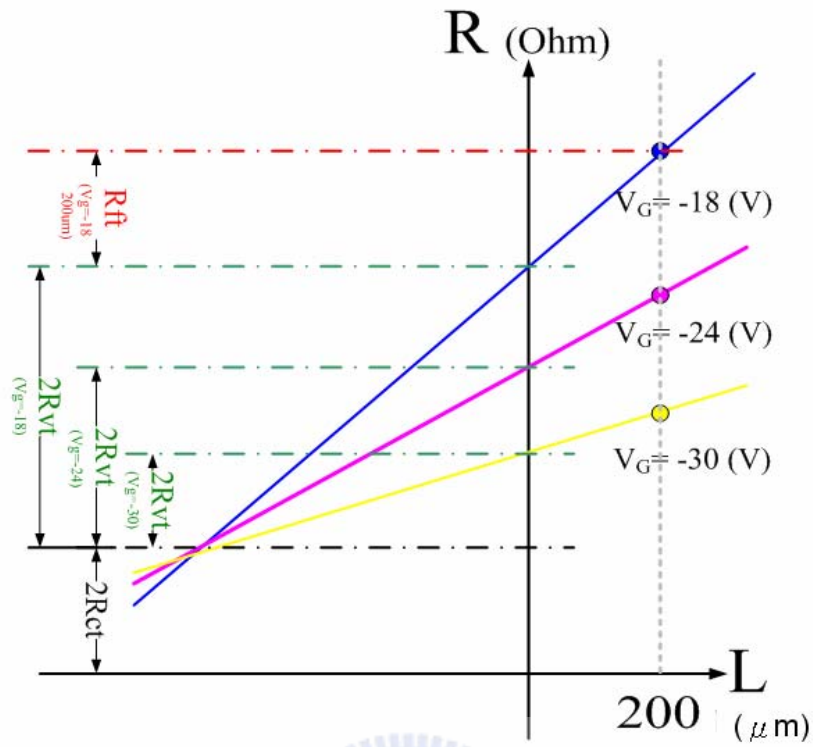


Fig. 3.13  $R_{ft}$ ,  $R_{vt}$ , and  $R_{ct}$  extraction and definition in TC OTFTs

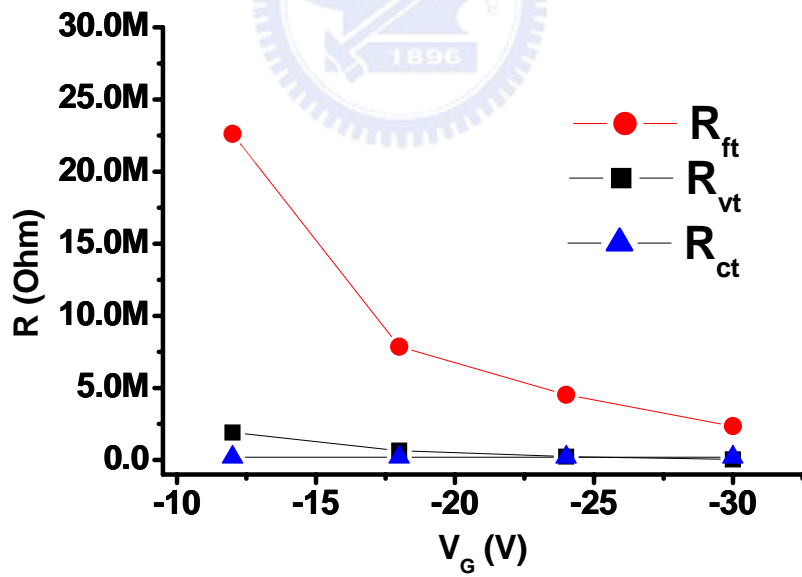


Fig. 3.14 Extracted resistances plotted as the function of gate-voltages in TC OTFTs

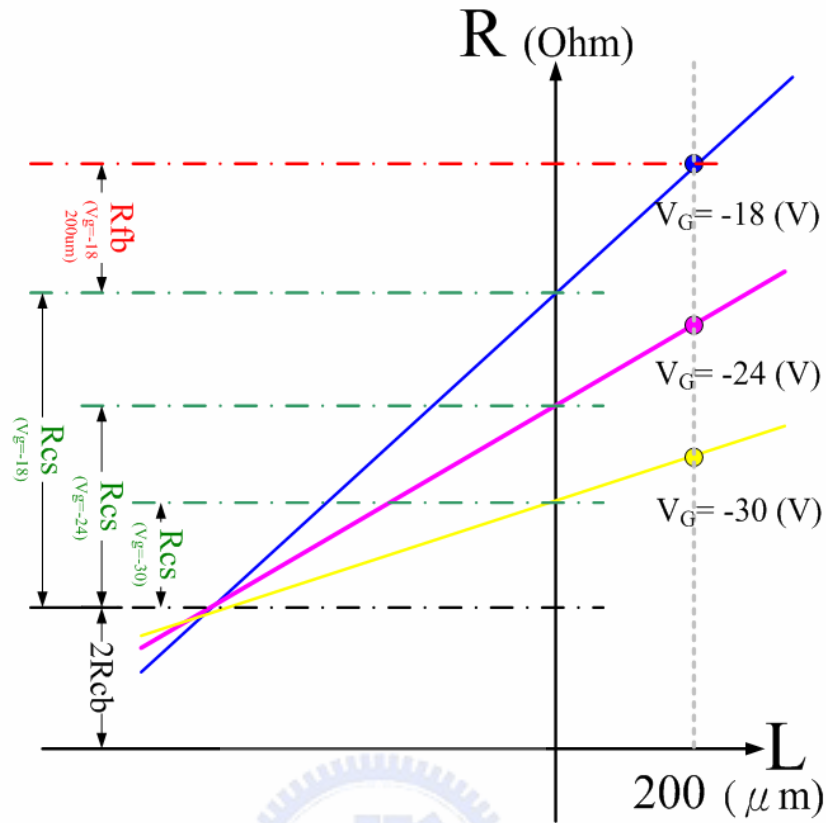


Fig. 3.15  $R_{fb}$ ,  $R_{cs}$ , and  $R_{cb}$  extraction and definition in BC OTFTs

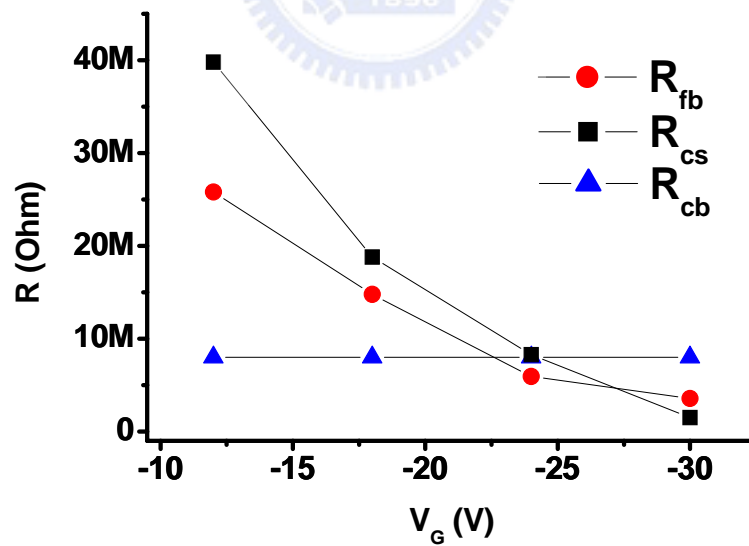
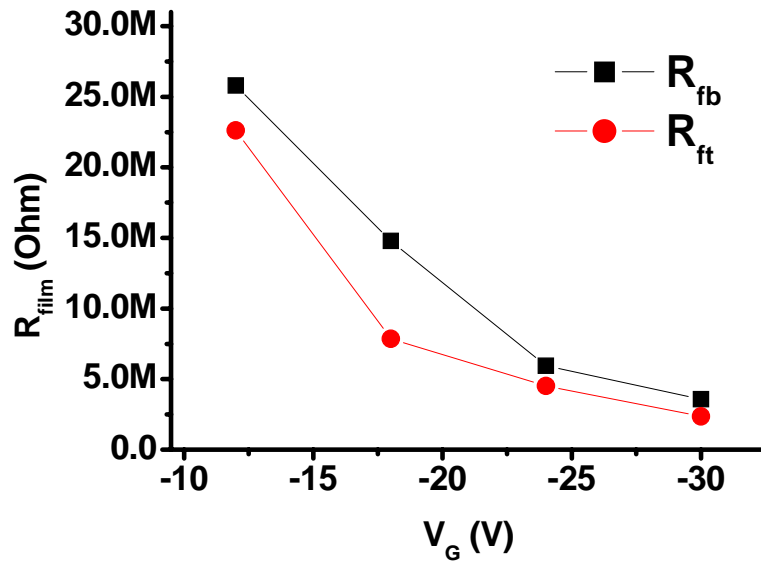


Fig. 3.16 Extracted resistance was plotted as a function of the gate-voltage in BC OTFTs



**Fig. 3.17** Film resistances from the TC OTFTs and the BC OTFTs are presented as the function of gate-voltage.

(a)

(b)

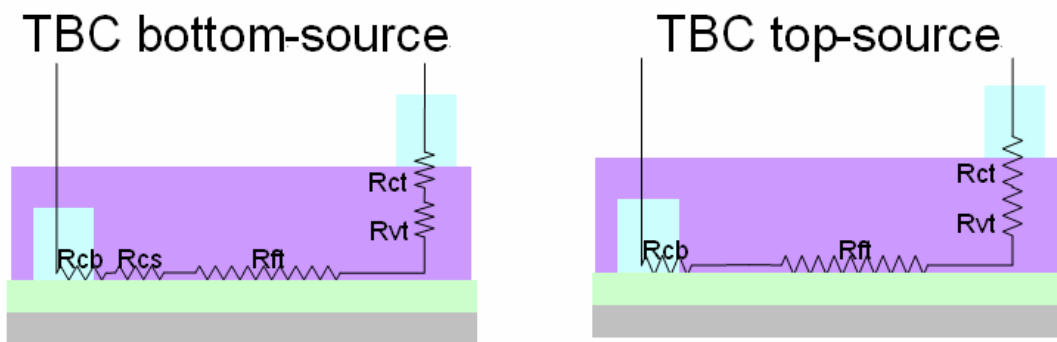
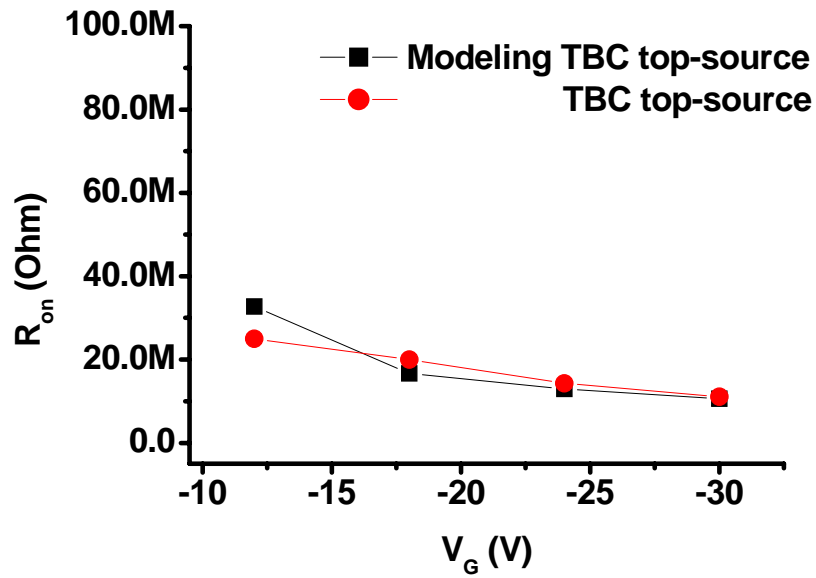


**Fig. 3.18**  $R_{on}$  modeling in (a) TBC bot-source (b) TBC top-source

(a)



(b)

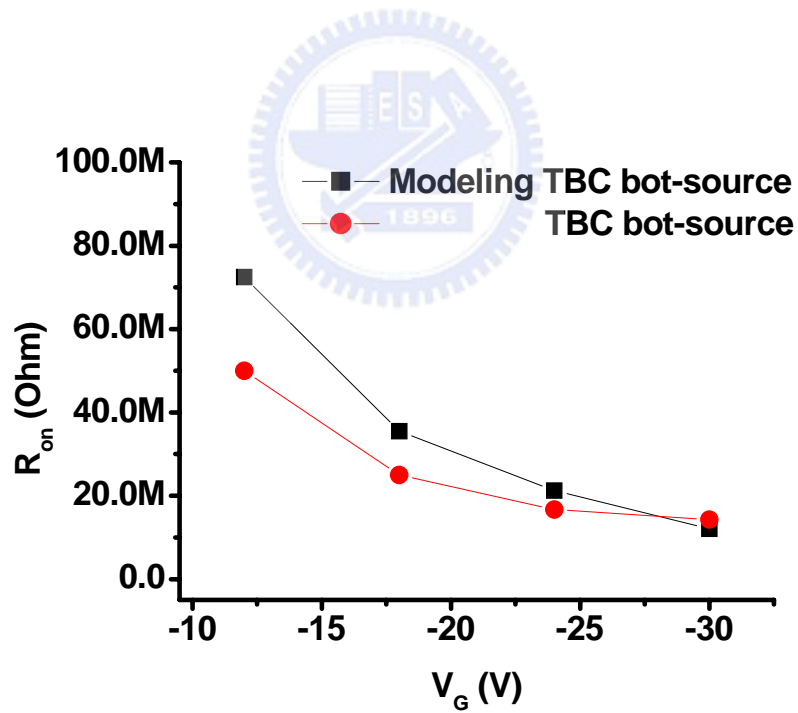


**Fig. 3.19** Total resistances from modeling and experiment are plotted (a) TBC bot-source (b) TBC top-source